Nonlinear Observer Design for PEM Fuel-Cell Systems using First-Order Sliding Mode Techniques

Zakaria BAROUD, Atallah BENALIA
Electrical Engineering Department,
LACoSERE Laboratory
Amar Telidji University,
Laghouat, Algeria.
E-mail: [z.baroud, a.benalia]@lagh-univ.dz

Carlos OCAMPO-MARTINEZ
Universitat Politècnica de Catalunya
Institut de Robòtica
i Informàtica Industrial (CSIC-UPC),
08028 Barcelona, Spain.
E-mail: cocampo@iri.upc.edu

***Abstract*—This paper presents a nonlinear observer design for Proton Exchange Membrane Fuel-Cell (PEMFC) systems. The aim of the proposed observer is to reconstruct the oxygen excess ratio through the estimation of their relevant states in real time from the measurement of the supply manifold air pressure. A First-Order Sliding Mode (FOSM) differentiation method is adopted to estimate, in finite time, the time derivative of the supply manifold air pressure. By means of the output-state inversion model, the relevant states are reconstructed. The objective of the proposed appproach is to minimize the use of additional sensors in order to reduce the costs and enhance the system accuracy. The performance of the proposed observer is analyzed through simulations considering measurement noise and different stack-current variations. The results show that the nonlinear observer properly estimates in finite time and robustly the oxygen excess ratio.**

***Index Terms*—PEM Fuel-Cell system, oxygen excess ratio, nonlinear observer, sliding mode differentiator.**

I. Introduction

The serious environmental pollution and energy crisis around the world are driving innovation on new efficient and clean energy sources such as solar, wind, geothermal and hydrogen. Fuel cells are a kind of clean energy, which produce electricity, water and heat from hydrogen and oxygen [1].

In particular, Proton Exchange Membrane fuel-cells (PEMFC), also called solid polymer fuel-cells (SPFCs), are considered to be more developed than other types of fuel-cells [2]. They are used in a wide range of applications, with advantages such as high efficiency, low weight, low pollution and low operation temperature, features that allow fast starting times in the PEMFC systems [3]. However, high expenses and short lifetime have hindered their massive utilization in real systems so far. As a result, advanced control systems are required to improve the lifetime and avoid the detrimental degradation of the PEMFC system.

One of the major problems in the PEMFC system is *oxygen starvation* when the stack-current increases rapidly. In order to avoid the oxygen starvation and to extend the life of the PEMFC system, many control strategies have been proposed to regulate fast and efficiently the oxygen depleted from the fuel-cell cathode. It can be cited, among others, linear control methods based on model linearization such as Linear Quadratic Regulator (LQR), proportional integral (PI) plus static feed-forward controllers proposed in [4] and [5], Second Order Sliding Mode (FOSM) based on super-twisting algorithm proposed in [6] and [7]. In [8] and [9], a hybrid controller based on fuzzy logic and conventional PID is designed. Nevertheless, all these control strategies require the knowledge of the precise value of oxygen excess ratio. Unfortunately, it depends on the internal variables corresponding to the partial pressures of oxygen and nitrogen in the cathode channel and the air pressure in the supply manifold. This means they should be measured by using extra sensors that increase the cost, the complexity and decreases the accuracy of the overall system. For these reasons, the estimation of the *observable states* using only the measurements of the available states becomes an attractive and economical solution.

Over the last decades, several studies have focused on the observer design for fuel-cell systems. Here, some available results are recalled: [10] proposed an approach to estimate the states of the PEMFC system using the Extended Kalman filter (EKF), based on a linearized model. In [11], a nonlinear state observer is designed by using the derivatives of the pressures at both cathode and anode. Moreover, [12] presented a finite time High-Order Sliding Mode (HOSM) observer to estimate some key states in a PEMFC system. In [13], an algebraic state observer is designed based on robust numerical differentiation of the supply manifold air pressure. These methods are applied for the estimation of the oxygen excess ratio in the PEMFC with different degrees of success.

In this paper, a nonlinear observer based on an FOSM differentiator is introduced to estimate state variables in the PEMFC system. The nonlinear observer allows the reconstruction of the system state variables in terms of inputs, outputs and their time derivatives up to some finite number. Thus, the accuracy and the robustness of the differentiaton method are the key elements of the observer design, a robust differentiation method based on [14] and [15] is used to estimate the time derivatives of output and input variables in finite time. The proposed observer estimates the partial pressures of oxygen and nitrogen from the measurements of the supply manifold air pressure.

The remainder of this paper is organized as follows. The

mathematical model of the PEMFC air supply system is briefly explained in Section II. In Section III, the design of the nonlinear observer is presented. Next, the proposed nonlinear observer is applied to the model of the PEMFC system and the simulation results for different stack-current changes and for noise in measurements are presented in detail in Section IV. Finally, the major conclusions are drawn in Section V.

II. Nonlinear PEMFC System Model

The PEMFC system includes five main sub-processes: the air flow (breathing), the hydrogen flow, the humidifier, the stack electrochemistry and the stack temperature. According to [16], it is considered that sufficient compressed hydrogen is available. In addition, it is assumed that both temperature and humidity of input reactant flows are properly regulated by dedicated local controllers, and thus the main regard is focused on the air management. Under these assumptions, a fourth-order state-space model is derived, which is a reduced version of the ninth-order model presented in [10].

The vector of states $x \in \mathbb{R}^4$ is associated to the partial pressure of oxygen and nitrogen in the cathode channel, the rotational speed of the motor shaft in the compressor and the air pressure in the supply manifold, respectively. The control input $u \in \mathbb{R}$ is the compressor motor voltage v_{cm}, which allows the manipulation of the air feed and, as a consequence, the oxygen supply to the fuel-cell stack. The measurable disturbance input $w \in \mathbb{R}$ is the stack-current I_{st}.

The governing equations for the previously described system states are given as follows [17]:

$$\frac{dx_1}{dt} = c_1\left(x_4 - \chi - c_2\right) - \frac{c_3 x_1 \alpha\left(x_1, x_2\right)}{c_4 x_1 + c_5 x_2 + c_6} - c_7 w, \tag{1}$$

$$\frac{dx_2}{dt} = c_8\left(x_4 - \chi - c_2\right) - \frac{c_3 x_2 \alpha\left(x_1, x_2\right)}{c_4 x_1 + c_5 x_2 + c_6}, \tag{2}$$

$$\frac{dx_3}{dt} = -c_9 x_3 - \frac{c_{10}}{x_3}\left(\left(\frac{x_4}{c_{14}}\right)^{c_{12}} - 1\right) y_3\left(x_3, x_4\right) + c_{13} u, \tag{3}$$

$$\frac{dx_4}{dt} = \phi\, c_{14}\left(1 + \left(c_{15}\left(\frac{x_4}{c_{11}}\right)^{c_{12}} - 1\right)\right), \tag{4}$$

with $\phi = \left(y_3\left(x_3, x_4\right) - c_{16}\left(x_4 - \chi - c_2\right)\right)$, where the constants $c_i, i \in [1, ..., 24]$ are defined in Table I in Appendix, the air cathode pressure, χ, is the sum of the oxygen and nitrogen partial pressures, namely x_1 and x_2. The cathode outlet mass flow rate, $\alpha(x_1, x_2)$, is expressed as follows:

$$\alpha(x_1, x_2) = c_{17}\left(\chi - c_2\right)\left(\frac{c_{11}}{\chi - c_2}\right)^{c_{18}} \sqrt{1 - \left(\frac{c_{11}}{\chi - c_2}\right)^{c_{12}}}. \tag{5}$$

The system output $y \in \mathbb{R}^3$, as illustrated in Figure 1, is the stack voltage $y_1 = V_{st}$, the supply manifold air pressure $y_2 = x_4$ and the air flow rate through the compressor $y_3 = W_{cp}$, respectively. The latter depends on the rotational speed of the motor shaft in the compressor and the air pressure in the supply manifold. For further details on the functions y_1 and y_3, see [10], [17] and [18].

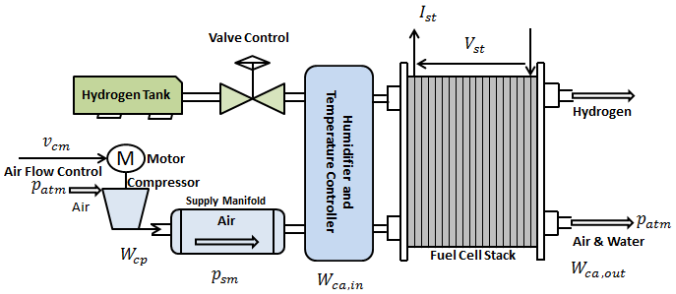

Figure 1: Fuel-Cell System showing control inputs and outputs

The performance variables $z \in \mathbb{R}^2$, with z_1 as the net power and z_2 as the oxygen excess ratio, are given as follows:

$$z_1 = y_1\left(x_1, x_2\right) w - c_{21} u\left(u - c_{22} x_3\right), \tag{6}$$

$$z_2 = \frac{c_{23}\left(x_4 - \chi - c_2\right)}{c_{24} w}. \tag{7}$$

In Section III, the nonlinear observer based on an FOSM differentiation method will be designed in order to estimate the oxygen excess ratio in the PEMFC system from the measurements of the input and outputs for the control purposes.

III. Nonlinear Observer design for the PEMFC system

This section is devoted to the nonlinear observer design for control purposes in the PEMFC system, as depicted in Figure 2. However, before to design the observer, the observability of the PEMFC system should be verified, which can be investigated by checking the observability rank condition. This latter is achieved according to [20]. The proposed observer is known for its finite time convergence and its robustness. In general, it is based on robust differentiation of outputs and inputs [15].

At the stage of controller design, it is needed to estimate the oxygen excess ratio, z_2. For this, it is needed to estimate firstly the sum of the oxygen and nitrogen partial pressures at the cathode channel, χ. The state $\hat{\chi}$ can be calculated using only the first derivative of the supply manifold air pressure x_4 and (4). Consider that the output $y_2 = x_4$ is a smooth function. An FOSM differentiator can be constructed for this signal as follows [15]:

$$\begin{cases} \dot{\xi}_1 = -\lambda_1 \mid e_1 \mid^{\frac{1}{2}} sign(e_1) + \xi_2, \\ \dot{\xi}_2 = -\lambda_2\, sign(e_1), \end{cases} \tag{8}$$

where $e_1 = \xi_1 - y_2$. Denote $e_2 = \xi_2 - \dot{y}_2$, system (8) can be rewritten as

$$\begin{cases} \dot{e}_1 = -\lambda_1 \mid e_1 \mid^{\frac{1}{2}} sign(e_1) + e_2, \\ \dot{e}_2 = -\lambda_2\, sign(e_1) - \ddot{y}_2, \end{cases} \tag{9}$$

with $|\ddot{y}_2| \leq L$, where L is an unkown positive constant and the gains λ_1 and λ_2 are formulated as

$$\begin{cases} \lambda_1 = 30 L^{\frac{1}{2}}, \\ \lambda_2 = 0.5 L. \end{cases} \tag{10}$$

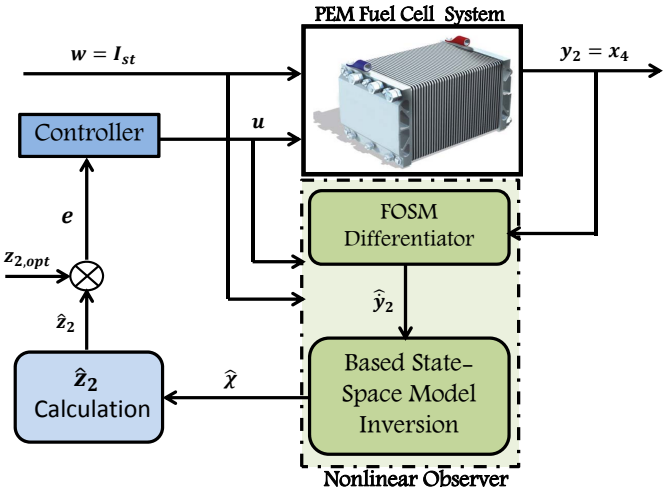

Figure 2: Nonlinear observer-based output-feedback control for the PEMFC system

Note that, in practice, the differentiator parameters λ_1 and λ_2 are often taken conservatively large to provide the best closed-loop performance in the presence of noises [15].

***Proposition** 1: Consider the error system (9). Suppose that gains λ_1 and λ_2 satisfy (10). Then, the states of the error system (9) converge to zero in finite time, i.e. $e_i = 0,\ i \in 1, 2$.*

Proof: The proof follows directly from [21]. ■

Proposition 1 implies that the states of the FOSM differentiator converge to their real values in finite time, respectively, i.e., $\xi_1 \to y_2$ and $\xi_2 \to \dot{y}_2$.

Then, one can obtain $\hat{\chi}$ from (4) and (8) as follows:

$$\hat{\chi} = \frac{1}{c_{16}} \left(\frac{\hat{\dot{y}}_2}{c_{14}\left(1 + \left(c_{15}\left(\frac{x_4}{c_{11}}\right)^{c_{12}} - 1\right)\right)} - y_3 \right) + x_4 - c_2. \quad (11)$$

The proposed observer is schematically shown in Figure 2, where $\hat{z}_2$ is estimated using $\hat{\chi}$ provided by the nonlinear observer and the nominal PEMFC parameters, defined in Table I in Appendix according to the following expression:

$$\hat{z}_2 = \frac{c_{23}\left(x_4 - (\hat{\chi} + c_2)\right)}{c_{24} w}. \quad (12)$$

IV. Simulation Results and Analysis

To assess the efficiency and the robustness of the nonlinear observer presented in Section III, detailed simulations are performed and analyzed. The numerical parameters used in the simulation are given in Table II in Appendix. At the time instant $t = 0$, the initial values $\xi_1(0) = x_4(0)$, $\xi_2(0) = 0$ were taken. The initial values of states are chosen as

$$x(0) = \left[\ 11104\,\text{Pa} \quad 83893\,\text{Pa} \quad 5100\,\text{rad/s} \quad 148000\,\text{Pa}\ \right]^T. \quad (13)$$

In the first place, the PEMFC system is supposed to be properly controlled as shown in Figure 2, where the controller adopted in this paper is taken directly from [19] to maintain the oxygen excess ratio at its optimal value $z_{2,opt}$.

A. Performance Results

The main purpose of the nonlinear observer design is to reconstruct the oxygen excess ratio in order to be useful for control purposes. The estimation of oxygen excess ratio value $\hat{z}_2$ under different stack-current variations (see Figure 3), using a nonlinear observer strategy is shown in Figure 4. It can be seen from Figure 4 that the nonlinear observer is perfectly able to reconstruct the value of oxygen excess ratio in finite time.

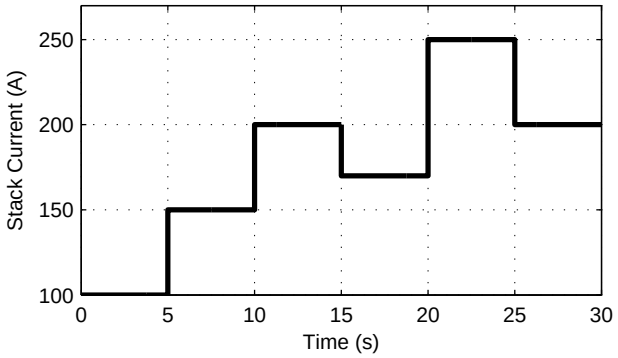

Figure 3: Stack-current variations

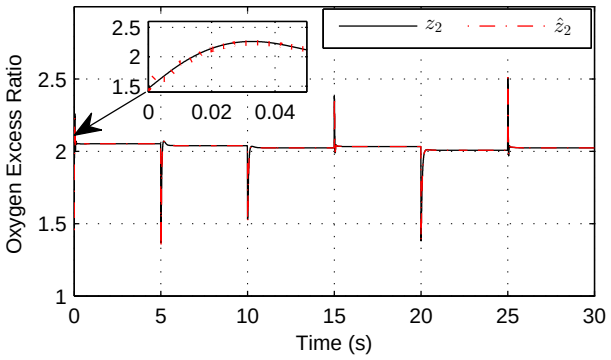

Figure 4: Estimation of z_2 under stack-current variations

Figure 5 presents the real and estimated values of χ under stack-current variations, which is well estimated based on the FOSM differentiation of the supply manifold air pressure. At the beginning of the estimation, the proposed observer reached the real values of χ in less than 40 ms.

B. Robustness test: Noise rejection

In order to test the robustness of the proposed observer, some simulations were carried out in the presence of measurement noise in y_2. Let $Y = y_2 + \theta$ be the real measurement of y_2, where θ is a white noise signal with mean $\mu = 9.4644 \times 10^{-4}$ and variance $\sigma^2 = 8.98022$.

The function θ used in the simulations is presented in Figure 6. The simulation results are shown in Figures 8 and 7. The

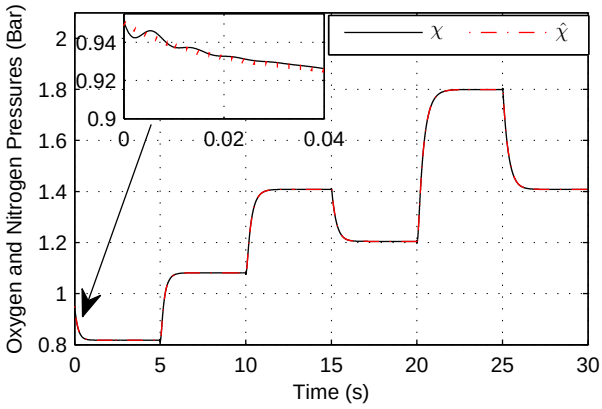

Figure 5: Estimation of χ under stack-current variation

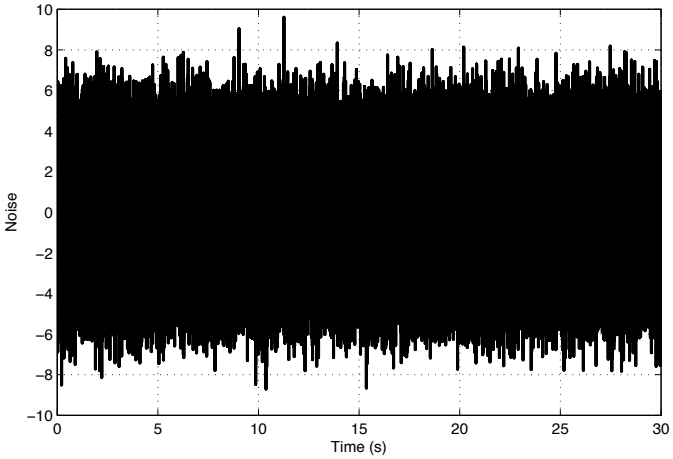

Figure 6: Noise θ affecting the system output y_2

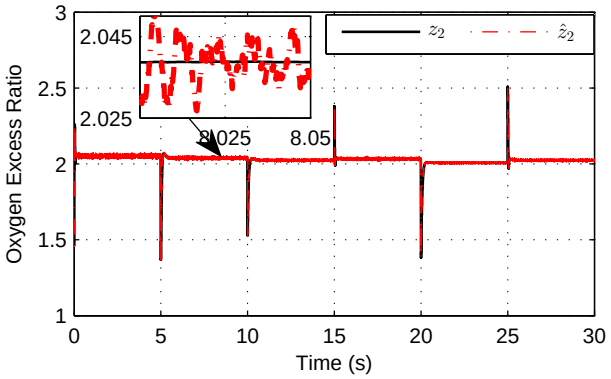

Figure 7: Estimation of z_2 under stack-currentvariations and measurement noise

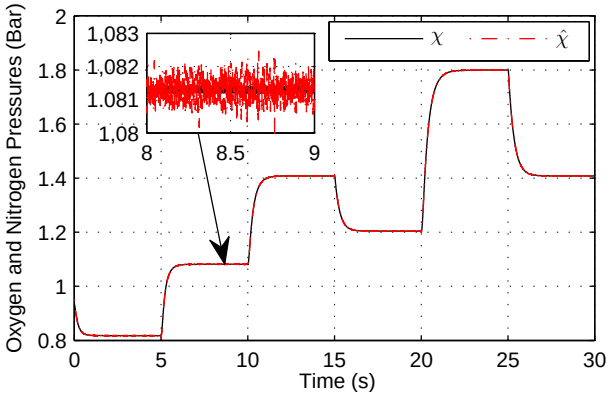

Figure 8: Estimation of χ under stack-currentvariations and measurement noise

oxygen excess ratio estimation under stack-current variations and measurement noise is depicted in Figure 7. In that figure, it is possible to see that the nonlinear observer estimates the oxygen excess ratio well enough in spite of the noise in the measurement.

V. Conclusion

In this paper, a nonlinear observer is designed to estimate the oxygen excess ratio. The proposed observer uses a robust differentiation method to estimate the derivative of the supply manifold air pressure in finite time. Then, the oxygen and the nitrogen partial pressures have been successfully estimated from the derivative estimated of the supply manifold air pressure. Simulation results show the robustness and the feasibility of the proposed observer. As future research, the applicability of the nonlinear observer will be confirmed in an experimental test bench.

References

[1] N. Yousfi-Steiner, P. Moçotéguy, D. Candusso, D. Hissel (2009) 'A review on polymer electrolyte membrane stack-current catalyst degradation and starvation issues: Causes, consequences and diagnostic for mitigation', *Journal of Power Sources* 194 (1) (2009) 130 – 145.

[2] Z. Baroud, M. Benmiloud, A. Benalia, C. Ocampo-Martinez (2017) 'Novel hybrid fuzzy-PID control scheme for air supply in PEM fuel cell-based systems', *International Journal of Hydrogen Energy*, 42 (15) (2011) 10435 - 10447.

[3] J. Larminie, A. Dicks, M. S. McDonald (2003) 'Fuel cell systems explained', Vol. 2, *Wiley New York*, 2003.

[4] J.T. Pukrushpan, A. Stefanopoulou, H. Peng (2004) 'Control of stack-current breathing', *IEEE, Control Systems*, 24 (2) (2004) 30–46.

[5] A. Niknezhadi, M. Allué-Fantova, C. Kunusch, C. Ocampo-Martinez (2011) 'Design and implementation of LQR/LQG strategies for oxygen stoichiometry control in PEM stack-currents based systems', *Journal of Power Sources*, 196 (9) (2011) 4277 – 4282.

[6] C. Kunusch, P. Puleston, M. Mayosky, J. Riera (2009) 'Sliding mode strategy for PEM stack-currents stacks breathing control using a super-twisting algorithm', *IEEE Transactions on Control Systems Technology*, 17 (1) (2009) 167–174.

[7] Z. Baroud, M. Benmiloud, A. Benalia (2015) 'Sliding mode controller for breathing subsystem on a PEM stack-current system', *3rd International Conference on Control and Engineering Information Technology (CEIT)*, 2015, pp. 1 – 6.

[8] Z. Baroud, M. Benmiloud, A. Benalia (2015) 'Fuzzy self-tuning PID controller for air supply on a PEM stack-current system', *4th International Conference on Electrical Engineering (ICEE)*, 2015, pp. 1–4.

[9] Z. Baroud, A. Benalia, C. Ocampo-Martinez (2016) 'Air Flow Regulation in Fuel Cell s: An Efficient Design of Hybrid Fuzzy-PID Control', *Electrotehnica, Electronica, Automatica (EEA)*, 64 (4) (2016) 28 – 32.

[10] J. Pukrushpan, A. Stefanopoulou, H. Peng (2004) 'Fuel Cell System Model: Fuel Cell Stack', *Control of Fuel Cell Power Systems, Springer London*, 2004.

[11] E. Kim (2012) 'Observer Based Nonlinear State Feedback Control

of PEM Fuel Cell Systems', *Journal of Electrical Engineering & Technology* 7 (6) (2012) 891 – 897.

[12] S.M. Rakhtala, A.R. Noei, R. Ghaderi, E. Usai (2014) 'Design of finite-time high-order sliding mode state observer: A practical insight to PEM stack-current system', *Journal of Process Control* 24 (1) (2014) 203 – 224.

[13] Z. Baroud, N. Gazzam, A. Benalia (2016) 'Algebraic Observer Design for PEM Fuel Cell System', *8th International Conference on Modelling, Identification and Control (ICMIC)*, Algiers, Algeria, 2016, pp. 1 – 5.

[14] A. Šabanović, K. Jezernik, N. Šabanović (2002) 'Sliding Modes Applications in Power Electronics and Electrical Drives', *Springer Berlin Heidelberg*, (2002) 223 – 251.

[15] Y. Shtessel, E. Christopher, F. Leonid L. Arie (2014) 'Sliding mode control and observation', *Springer*, (2014) XVII – 356.

[16] K. W. Suh (2006) 'Modeling, analysis and control of stack-current hybrid power systems', *Ph. D. thesis* (2006).

[17] J. Gruber, C. Bordons, F. Dorado (2008) 'Nonlinear control of the air feed of a stack-current', *American Control Conference*, 2008, pp. 1121–1126.

[18] Z. Baroud, M. Benmiloud, A. Benalia (2014) 'Modelling and Analysis of Proton Exchange Membrane Fuel Cell System', *3rd International Conference on Information Processing and Electrical Engineering (ICIPEE)*, Algiers, Algeria, 2014, pp. 1 – 6.

[19] Z. Baroud, A. Benalia, C. Ocampo-Martinez (2017) 'Robust Fuzzy Sliding Mode Control For Air Supply on PEM Fuel Cell System', *International Journal of Modelling, Identification and Control*, 2017, Accepted for publishing.

[20] J. Liu, S. Laghrouche, M. Wack (2013) 'Differential flatness-based observer design for a PEM stack-current using adaptive-gain sliding mode differentiators', *European Control Conference (ECC)* (2013), Zurich, 2477-2482.

[21] J. Liu, S. Laghrouche, Z.S. Ahmed, M. Wack (2015) 'PEM stack current air-feed system observer design for automotive applications: An adaptive numerical differentiation approach', *International Journal of Hydrogen Energy* 39 (30) (2014) 17210 – 17221.

APPENDIX

Table I: Constants of the PEMFC system model

$$c_1 = \frac{RT_{st}k_{ca,in}}{M_{O_2}V_{ca}}\left(\frac{x_{O_2,atm}}{1+\omega_{atm}}\right)$$
$$c_2 = p_{sat}$$
$$c_3 = \frac{RT_{st}}{V_{ca}}$$
$$c_4 = M_{O_2}$$
$$c_5 = M_{N_2}$$
$$c_6 = M_v p_{sat}$$
$$c_7 = \frac{RT_{st}n}{4FV_{ca}}$$
$$c_8 = \frac{RT_{st}k_{ca,in}}{M_{N_2}V_{ca}}\left(\frac{1-x_{O_2,atm}}{1+\omega_{atm}}\right)$$
$$c_9 = \frac{\eta_{cm}k_t k_v}{J_{cp}R_{cm}}$$
$$c_{10} = \frac{C_p T_{atm}}{J_{cp}\eta_{cp}}$$
$$c_{11} = p_{atm}$$
$$c_{12} = \frac{\gamma-1}{\gamma}$$
$$c_{13} = \frac{\eta_{cm}k_t}{J_{cp}R_{cm}}$$
$$c_{14} = \frac{RT_{atm}\gamma}{M_{a,atm}V_{sm}}$$
$$c_{15} = \frac{1}{\eta_{cp}}$$
$$c_{16} = k_{ca,in}$$
$$c_{17} = \frac{C_D A_T}{\sqrt{RT_{st}}}\sqrt{\frac{2\gamma}{\gamma-1}}$$
$$c_{18} = \frac{1}{\gamma}$$
$$c_{19} = \left(\frac{2}{\gamma+1}\right)^{\frac{\gamma}{\gamma-1}}$$
$$c_{20} = \frac{C_D A_T}{\sqrt{RT_{st}}}\gamma^{0.5}\left(\frac{2}{\gamma+1}\right)^{\frac{\gamma+1}{2\gamma-2}}$$
$$c_{21} = \frac{1}{R_{cm}}$$
$$c_{22} = k_v$$
$$c_{23} = k_{ca,in}\left(\frac{x_{O_2,atm}}{1+\omega_{atm}}\right)$$
$$c_{24} = \frac{nM_{O_2}}{4F}$$
$$x_{O_2,atm} = \frac{y_{O_2,atm}M_{O_2}}{M_{a,atm}}$$
$$\omega_{atm} = \frac{M_v}{M_{a,atm}}\frac{\phi_{atm}p_{sat}}{p_{atm}-\phi_{atm}p_{sat}}$$

Table II: Simulation Parameters

Parameter	Description	Value	Unit
η_{cp}	Motor mechanical efficiency	0.98	%
η_{cm}	Compressor efficiency	0.8	%
J_{cp}	Compressor inertia	5×10^{-5}	kg m^2
R_{cm}	Compressor motor resistance	0.82	Ω
k_t	Motor parameter	0.0153	(N m)/A
k_v	Motor parameter	0.0153	V/(rad/s)
$M_{a,atm}$	Air molar mass	29×10^{-3}	kg mol^{-1}
M_{O_2}	Oxygen molar mass	32×10^{-3}	kg mol^{-1}
M_{N_2}	Nitrogen molar mass	28×10^{-3}	kg mol^{-1}
M_v	Vapor molar mass	18×10^{-3}	kg mol^{-1}
$y_{O_2,atm}$	Oxygen mole fraction	0.21	–
V_{ca}	Cathode volume	0.01	m^3
$k_{ca,in}$	Cathode inlet orifice constant	0.3629×10^{-5}	kg/(s Pa)
V_{sm}	Supply manifold volume	0.02	m^3
T_{st}	Stack temperature	353.15	K
T_{atm}	Atmospheric temperature	298.15	K
p_{atm}	Atmospheric pressure	101325	Pa
p_{sat}	Saturation pressure	465327.41	Pa
R	Universal gas constant	8.3145	J/(mol K)
C_p	Constant pressure Specific heat of air	1004	J/(mol K)
C_D	Cathode outlet throttle discharge coefficient	0.0124	–
γ	Ratio of specific heat of air	1.4	–
A_T	Cathode outlet throttle area	0.002	m^2
ϕ_{atm}	Average ambient air relative humidity	0.5	–
n	Number of cells in fuel-cell stack	381	–
F	Faraday number	96485	C mol^{-1}